

# REPORT DOCUMENTATION PAGE

Form Approved  
OMB No. 0704-0188

Public reporting burden for this collection of information is estimated to average 1 hour per response, including the time for reviewing instructions, searching existing data sources, gathering and maintaining the data needed, and completing and reviewing this collection of information. Send comments regarding this burden estimate or any other aspect of this collection of information, including suggestions for reducing this burden to Department of Defense, Washington Headquarters Services, Directorate for Information Operations and Reports (0704-0188), 1215 Jefferson Davis Highway, Suite 1204, Arlington, VA 22202-4302. Respondents should be aware that notwithstanding any other provision of law, no person shall be subject to any penalty for failing to comply with a collection of information if it does not display a currently valid OMB control number. PLEASE DO NOT RETURN YOUR FORM TO THE ABOVE ADDRESS.

1. REPORT DATE (DD-MM-YYYY)

2. REPORT TYPE  
Technical Papers

3. DATES COVERED (From - To)

4. TITLE AND SUBTITLE

5a. CONTRACT NUMBER

5b. GRANT NUMBER

5c. PROGRAM ELEMENT NUMBER

6. AUTHOR(S)

5d. PROJECT NUMBER  
1011

5e. TASK NUMBER  
0062

5f. WORK UNIT NUMBER

7. PERFORMING ORGANIZATION NAME(S) AND ADDRESS(ES)

Air Force Research Laboratory (AFMC)  
AFRL/PRS  
5 Pollux Drive  
Edwards AFB CA 93524-7048

8. PERFORMING ORGANIZATION  
REPORT

9. SPONSORING / MONITORING AGENCY NAME(S) AND ADDRESS(ES)

Air Force Research Laboratory (AFMC)  
AFRL/PRS  
5 Pollux Drive  
Edwards AFB CA 93524-7048

10. SPONSOR/MONITOR'S  
ACRONYM(S)

11. SPONSOR/MONITOR'S  
NUMBER(S)

12. DISTRIBUTION / AVAILABILITY STATEMENT

Approved for public release; distribution unlimited.

13. SUPPLEMENTARY NOTES

14. ABSTRACT

20021119 056

15. SUBJECT TERMS

16. SECURITY CLASSIFICATION OF:

17. LIMITATION  
OF ABSTRACT

18. NUMBER  
OF PAGES

19a. NAME OF RESPONSIBLE  
PERSON

Leilani Richardson

19b. TELEPHONE NUMBER  
(include area code)  
(661) 275-5015

a. REPORT

b. ABSTRACT

c. THIS PAGE

Unclassified

Unclassified

Unclassified

A

Standard Form 298 (Rev. 8-98)  
Prescribed by ANSI Std. Z39.18

6 Separate items are enclosed

MEMORANDUM FOR IN-HOUSE PUBLICATIONS

FROM: PROI (TI) (STINFO)

11 Jun 98

SUBJECT: Authorization for Release of Technical Information, Control Number: AFRL-PR-ED-TP-1998-111  
Stephanie Chenault "Engine Optimization for a Solar Thermal Powered Orbit Transfer Vehicle"  
(Statement A)

---

# **Engine Optimization for A Solar Thermal Powered Orbit Transfer Vehicle**

Stephanie Renee Chenault  
Air Force Research Laboratory  
Edwards AFB, CA

## **Abstract**

Recent technological advancements in solar thermal rocket propulsion and solar orbit transfer vehicles make it critical to perform additional engine performance analyses. Several system level flight demonstrations are imminent. Space flight hardware component testing is being conducted at the Air Force Research Laboratory, Edwards AFB, California. The focus of current research is engine and nozzle configurations for a solar orbit transfer vehicle. The optimal design must produce 1-10 pounds thrust, perform at high Isp and be compatible in a hybrid of spiral, perigee, and apogee (multi-burn) configurations. The nozzle material must not ablate when subjected to extreme thermal loading, yet be durable enough to withstand widely varying temperature differentials during frequent thermal cycling. This paper addresses propulsive needs in the orbit transfer arena and defines governing upper stage vehicle engine equations. These equations are modified versions of rocket engine equations used for chemical systems. The correction factors and modifications are for Solar Thermal Propulsion specific hardware.

## **Introduction**

Solar Thermal Propulsion (STP) uses large parabolic off-axis mirrors to focus sunlight into an absorber-heat exchanger. The solar concentrators transfer a minimum of 3000 K into the propellant (Fig. 1). A blackbody absorber is a heat-transferring engine that will not emissively degrade the incoming solar flux. Gaseous hydrogen propellant is directed from an inlet and distributed throughout the heat-exchanging cavity. Hydrogen gas, used for its low molecular weight, must be channeled through the absorber walls because it is largely transparent to sunlight, and will not absorb heat on its own. This heat transfer process allows the hot hydrogen to be thermodynamically expanded through a nozzle located aft of the engine absorber. This propulsion concept is simple and effective.

The current fleet of spacecraft in the US inventory can place less than 1% of their total launch mass into high orbits. The United States Air Force is continually exploring innovative propulsion concepts, such as STP, to place military payloads into space reliably at lower cost. Ground demonstrations have proven the capability of engine performance and concentrator/strut deployment. An upcoming flight test experiment will validate STP's performance potential as a reliable orbit transfer vehicle.

**DISTRIBUTION STATEMENT A:**  
Approved for Public Release -  
Distribution Unlimited

---

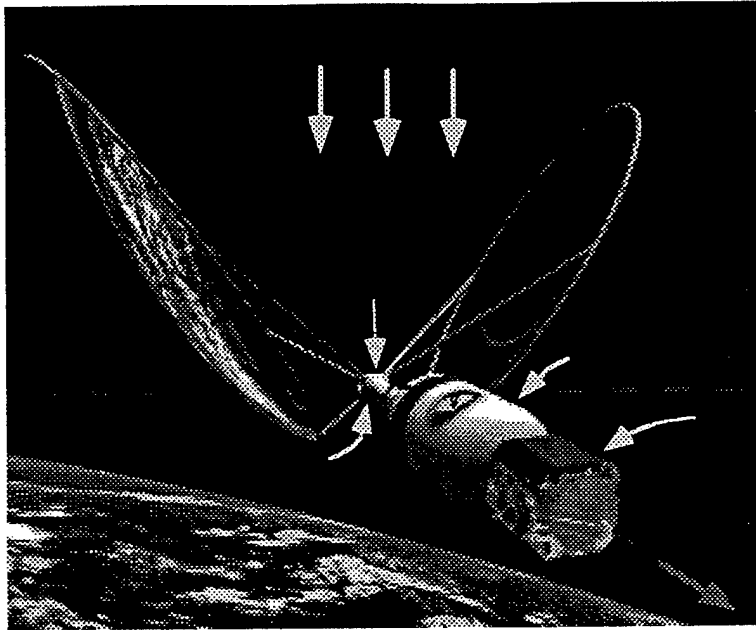


**Figure 1. STP System Hardware**

A Low Earth Orbit (LEO) to Geosynchronous Earth Orbit (GEO) transfer vehicle (upper stage) must exceed current vehicle performance levels if it is to replace traditional (chemical and electrical) rocket systems. Although high specific impulse (Isp) reduces propellant mass, it compromises thrust levels. Trade-off studies prove that the propellant storage volume saved would enable more payload to be manifested in a launch vehicle shroud with only a moderate increase in trip time. For a typical solar orbit transfer trip time would be 30 days for a multi-burn transfer, utilizing a hybrid of perigee and apogee burns. To effectively reach the GEO altitude, the spacecraft must perform roughly 10 times as many perigee as apogee burns (Fig. 2).

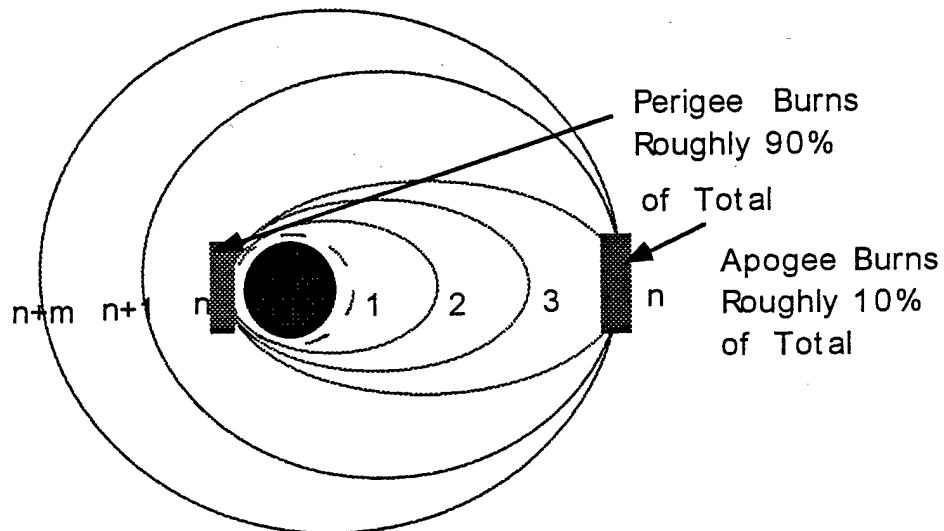


**Figure 2. Transfer Type for 30-Day Trip Time**

## The Basic Solar Engine

The basic solar engine offers substantial performance efficiency improvements over traditional chemical rocket performance. Chemical rockets, which have the energy source coincident with the propellant, are fundamentally limited in their achievable specific impulse by the strength of the chemical bonds of the propellant ( $I_{sp} = 450s$ ). If high specific impulses are to be achieved, an energy source other than, or in addition to, the propellant must be used. The solar concentrators serve this purpose for a STP without having to use combustion.

The two most important rocket engine performance parameters are thrust and  $I_{sp}$ . Thrust is the final velocity of the propellant times the mass flow rate out of the nozzle. The solar engine operates by expanding hot hydrogen gas and accelerating it to produce thrust. Thrust is then divided by the total propellant mass flow rate to determine  $I_{sp}$ . Using basic rocket propulsion equations we can solve for these parameters:

$$P_{thrust} = 1/2 \dot{m} v_{exit}^2 \quad (1)$$

Equation 1 shows how the mass flow rate is related to power ( $P_{thrust}$ ), while Equations 2 and 3 present the basic definitions of  $I_{sp}$  and thrust.

$$F = \dot{m} v_{exit} + \dot{m} v_{dot exit} \quad or \quad F = \dot{m} v_{exit} + \Delta P_{exit} A_{exit} \quad (2)$$

$$\therefore I_{sp} (g) = F / \dot{m} \quad or \quad P_{thrust} = 1/2 F I_{sp} (g) \quad (3)$$

These equations work fairly well for defining ideal rocket engine performance; unfortunately several key and uncommon factors must be addressed which play a significant role in designing an optimal solar engine. For example, boundary conditions and thermal losses for flowing hot, corrosive hydrogen through a blackbody absorber need to be considered, and the governing equations must be modified to accommodate these changes.

## Why Basic Rocket Equations Fail Solar

As propellant hydrogen is lightweight, cryogenically storable, and ideal for STP propulsive needs. However, when heated to extremely high temperature (3000 K), dissociation of diatomic hydrogen molecules becomes a concern. From a thermodynamic standpoint, the rate at which  $H_2$  is dissociated into H will not affect the ratio of specific heat ( $\gamma$ ). This is because the rate of dissociation is sufficiently small enough at these temperatures that the ratio of specific heats is essentially constant.

When the propellant is expelled through a rocket nozzle with no further chemical reaction, the flow is said to be "frozen". If frozen flow is assumed (for traditional propulsion equations), the mixture of these two gases, diatomic and monatomic, will not change as it is accelerated through the engine. However, more accurately, the energy used to disjoin the hydrogen is conserved by the recombination of H into  $H_2$  along the nozzle surfaces. Although this operation returns some of the energy to the gas, it creates a boundary layer thrust loss and reduces  $I_{sp}$ .

The blackbody radiator employed by STP raises some important performance analysis and sizing concerns. Thermal losses and power drops must be accounted for in new thrust and  $I_{sp}$  equations to optimize the engine design. The correction factor that accounts for power losses,  $\tau_{eff}$ , is a measure of efficiency. Total efficiency is a sum of the internal efficiency,  $\eta_{int}$ , and the propulsive efficiency,  $\eta_p$ . For solar propulsion  $\eta_{int}$  is assumed to be 0.50. This factor can be placed within the governing rocket equations. Also the *effective exhaust velocity*,  $c$ , is used instead of the ideal exhaust velocity,  $v_{exit}$ , to incorporate these losses. The efficiency of the engine,  $\tau_{eff}$ , encompasses thrust vector loss along the rocket axis (quantified by the cosine of the nozzle angle) and overall nozzle power loss. The nozzle angle is defined in Figure 3 as alpha. The nozzle used for STP is a converging/diverging nozzle.

Equations 4-7 account for losses that are generally disregarded during the design process for chemical systems. This is not to suggest that chemical propulsive systems do not encounter significant performance drops due to power losses; quite the opposite, chemical systems must deal with possibly greater net losses due to the complexities associated with combustion. While the inclusion of efficiency terms may lead to a more closely traceable STP system, the values attributed to these terms must be analytically determined and then validated through experimental testing. It is through extensive "ground" engine testing that actual vs. real thrust/ Isp levels can be quantified.

$$\tau_{\text{eff}} = \eta_{\text{int}} + \eta_p \quad (4)$$

$$P_{\text{thrust}} = \tau_{\text{eff}} \Delta h \dot{m}_{\text{dot}} / \mu = 1/2 F \text{ Isp (g)} \quad (5)$$

$$1/2 F \text{ Isp (g)} = 1/2 \dot{m}_{\text{dot}} c^2 \quad (6)$$

$$\therefore \text{Isp} = 1/g (2 \tau_{\text{eff}} \Delta h \dot{m}_{\text{dot}} / \mu) \quad (7)$$

The nozzle power loss is defined as 5%. Therefore, the effective velocity used in Equation 6 can be solved using Equation 8. The subscripts used to denote location along the thrust axis of the engine are shown in Figure 3. The effective velocity,  $c$ , is defined by:

$$c = v_2 + (p_2 - p_3) A_2 / \dot{m}_{\text{dot}} \quad (8)$$

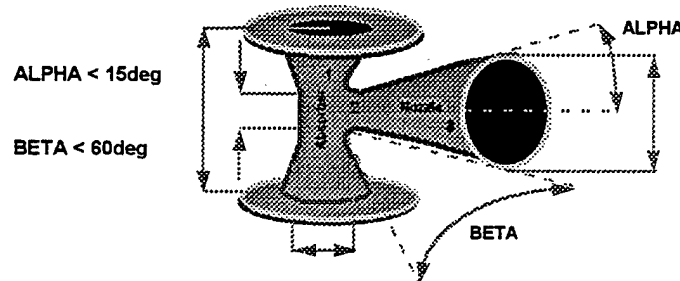


**Figure 3. Subscript Location and Characteristic Angle Design Criteria**

Change in enthalpy,  $\Delta h$ , must include thermodynamic losses. The parameter  $\Delta h = h_{\text{absorber exit}} - h_{\text{thrustor exit}}$ . The heat of formation is defined as the positive interaction required to form the original composition from its products ( $\text{H}$  and  $\text{H}_2$ ) at a constant pressure and prescribed temperature. For the STP case, the heat of formation refers to the amount of dissociated hydrogen present in the total propellant mass as a result of expansion and heating. In Equation 9 this is represented by:

$$\Delta h = \sum n_2 \Delta h_2^\circ - \sum n_3 \Delta h_3^\circ \quad (9)$$

where the subscripts 2 and 3 describe whether this value is taken prior or after full expansion within the engine (leaving the absorber or leaving the thruster),  $n$  is the number of moles and  $\Delta h$  is the heat of formation per mole.

Solving Equation 9 yields the following:

- 1.) Clarifies why real vs. theoretical number divergence occurs,
- 2.) Enables more reliable thermal modeling, and
- 3.) Reduces the number of iterations required to produce acceptable performance levels for future designs that meet mission. These equations set the baseline for STP design criteria.

## The Design Process

This section presents the detailed equations used to design our STP engines. Since our engine does not require combustion, only high temperature losses need to be considered. There are no combustion or chemical losses present in a STP system. Since the designer is aware of the performance values ( $I_{sp}$  and  $T$ ) needed to meet mission requirements, designing a STP engine is a simple, executable process.

To determine nozzle size used for given engine-operating conditions, important temperatures and pressures must first be calculated, and then measured experimentally. Equations 10-13 theoretically determine the temperatures and pressures extracted from chamber/absorber conditions related to the nozzle throat. The theoretical values for these actual conditions should be confirmed experimentally. The solar laboratory facility supplies the means to measure the calculated values using thermocouples and pressure transducer input to data acquisition hardware/software. This allows the experimenter to actively monitor the test engine and insure that it is operating under its design parameters.

$T_2$  is the temperature of the hydrogen gas at the nozzle throat. It is given by Equation 10:

$$T_2 = T_1 [1 / (1 + (\gamma - 1) / 2)]. \quad (10)$$

The ratio of specific heats,  $\gamma$ , is equal to the nondimensional value 1.4 (even when the hydrogen propellant is subjected to extremely high temperatures). This yields a throat temperature of:

$$T_2 = 0.833 T_1 \quad (11)$$

where  $T_1$  is the absorber chamber temperature given in degrees Rankine ( $^{\circ}R$ ). With an absorber temperature of  $3600^{\circ}R$ , the throat temperature then can be derived.

$P_t$  is the hydrogen gas pressure at the throat. The pressure at this location is less than the chamber pressure, due to the acceleration of the gas through the engine. The value for  $P_t$  is given by:

$$P_2 = P_1 [1 + (\gamma - 2) / 2]^{-\gamma / (\gamma - 1)}. \quad (12)$$

The chamber pressure is typically set at 150 psia for STP applications. This value,  $g$ , was experimentally validated in conditions that met the limitations and mass flow requirements defined in Equation 6. Inserting this value for  $g$  into Equation 8 gives:

$$P_2 = 0.528 P_1. \quad (13)$$

To obtain maximum thrust, the hot hydrogen gas must be expanded in the diverging section of the nozzle. Since the amount of energy needed to accelerate the hydrogen creates a net pressure drop through the nozzle, the next step in the design process is to locate the exact location where the gas pressure is equal to the local atmospheric pressure. This area which is denoted by the subscript 3 in Figure 3 is commonly called the nozzle exit area.

First, to define the exit area of the nozzle, the Mach number must be found. The Mach number is the ratio of the velocity of the gas to the local speed of sound. The perfect gas expansion expression can be used since our engine involves no combustion.

$$M_3^2 = 2 / (\gamma - 1) [(p_1 / p_3)^{(\gamma - 1) / \gamma} - 1] \quad (14)$$

$P_3$  is the value of the pressure at the nozzle exit plane. For a STP system in LEO, a good approximation of  $p_{atm}$  is 0.2 psia due to plume interaction or backflow. The nozzle cannot be fully expanded and its length must be truncated to discourage flow separation along the nozzle walls, and subsequent shock development. It has also been numerically determined that an overall nozzle area ratio (exit to throat) be assumed to be 50:1. Once the Mach number is calculated,

determining the geometric qualities of the operating system can begin. The exit area and the throat area are given in Equation 15:

$$A_3 = A_2/M_3 [1 + ((\gamma-1)/2) M_3^2 / ((\gamma-1)/2)]^{(\gamma+1)/2(\gamma-1)} \quad (15)$$

where

$$A_2 = m_{\text{dot}} / p_2 (R T_2 / (\gamma g_c))^{1/2}. \quad (16)$$

Solving for  $m_{\text{dot}}$  using the corrected Equation 7 yields a propellant flow rate of 0.002 lb. per second. The throat area is then calculated. Using Equation 10 we find the exit area. Note that the area expansion ratio is usually prescribed to be 50:1. Using typical STP operating pressures and temperatures (150 psia and 3600°R) the actual expansion ratio is 32:1. Solve Equations 10 and 11 to calculate the diameter of the orifices. While these equations take into consideration power losses due to propellant and propulsive inefficiencies; they do not account for boundary layer accumulation or flow divergence. The next section will deal with boundary layer effects and characteristic lengths of the engine. Since the nozzles are designed to be underexpanded, there is no accumulation of shock waves within the cone of the diverging/converging nozzle.

### Boundary Layer Generation

The throat area and the nozzle exit area have been calculated using a mass flow rate that incorporates power losses by the engine. While these results are suitable for designing an engine, it is important to calculate the boundary layer associated with the flow, even though the losses associated with boundary layer development are typically only 1-10% of total flow area. For larger systems, this is significant because only approximately 90% of the flow remain undisturbed as it is accelerated and expanded through the engine. The boundary layer is calculated by:

$$\delta_b = 0.16x / (Re_x)^{1/4}. \quad (17)$$

For turbulent flow the Reynolds number ( $Re_x$ ) is given by:

$$Re_x = v_x / \nu \quad \text{where} \quad v_x = [(2 g_c \gamma R T_1) / (\gamma + 1)]^{1/2}. \quad (18)$$

The thermal expansion correction factor is given by:

$$\delta_{th} = \alpha (\Delta T) L. \quad (19)$$

In Equation 15 alpha ( $\alpha$ ) is material specific and  $\Delta T$  is experimentally obtained. These two parameters are then multiplied by nozzle length (L). Nozzle length for STP would be the length along the thrusting axis starting at the absorber exit plane ending at the engine exit plane. Note the length of the nozzle must be truncated to discourage flow separation and shock formation.

The final correction factor relates the change in the nozzle's effective circumference due to pressure effects. This last correction factor also includes stress effects:

$$\sigma = (P_2 - P_3) r / t. \quad (20)$$

In this equation, sigma ( $\sigma$ ), is a function of throat and exit pressure in conjunction with thickness and nozzle throat radius. The radius,  $r$ , is the actual radius without any correction factor. The final radius will be calculated from the sum of these losses. The thickness of the material,  $t$ , is also a known parameter. It is determined by the availability of the material used (typically tungsten, rhenium, molybdenum) and material requirements (see Equation 15). The value that is calculated for  $\sigma$  can then be related to an actual lessening of circumference in Equation 21.

$$\delta_{cir} = \sigma L / E \quad (21)$$

where E is the modulus and is a material specific value. The change in the circumference can then be converted to a change in diameter. The total correction in the throat diameter is found by the summation of all of the correction values:

$$\delta_{tot} = \delta_{cir} + \delta_b = \delta_{th}. \quad (22)$$

Equation 22 may now be applied to the throat diameter. This correction equation includes the boundary layer, thermal expansion and pressure influence.

While it is not much of technical challenge to use modified equations to produce an engine that meets specific mission requirements, actually fabricating and testing the designed engine may prove to be difficult. For low-level thrust requirements typically the "nozzle" employed has been a bored-out hole aft of the absorber. This method works reasonably for chamber tests (order of  $1 \times 10^{-6}$  torr), but is not optimal for space-rated hardware. Special fabricating procedures must be practiced. Precise equipment, preferably machinery used in conjunction with a CAD package, is mandatory to meet the tolerances required for a STP system.

Once the engine has been built to specifications, testing may be initiated. In the ideal scenario, thrust measurements taken during the tests will reinforce numerical estimates. Unfortunately, there is no foolproof method for achieving the same numbers experimentally as analytically. It is evident that while these equations help reduce engine performance uncertainty, they promise no guarantee for performance results. The most equitable method for ensuring rocket performance is to test with the correction factor iterations until discrepancies can be identified and corrected.

Each engine that will be used for STP will change with changed mission requirements. For example, where one mission may require a simple orbit transfer of a satellite, another may be specified to execute a deep space probe. Chemical propulsion systems are currently reaching mission limitations due to high fuel requirements and propellant storage limitations. If deep space missions are to continue, an earth-to-orbit chemical propulsion system with a high Isp upper stage must be used to lower launch costs and reduce lift-off weight. The solar group plans to test a variety of engines to meet USAF propulsive upper-stage needs and share the technology they develop with the commercial launch vehicle industry.

## Conclusions

Most of the engines tested in the solar laboratory have been designed and fabricated by government contractors as deliverables in SBIR (small business innovative research) contracts. After an engine is produced, it is shipped to the Solar Lab where it undergoes on-sun testing with a ground-based concentrator. A data acquisition system monitors characteristic pressures and temperatures and relates them to performance values. (For typical test results see Figure 4.)

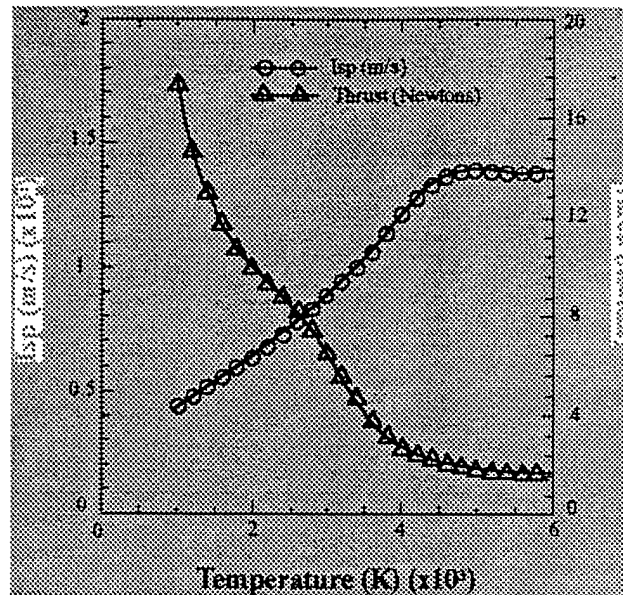


**Figure 4. Relationship between Thrust, Temperature and Isp**

Some members of the solar group also design and build engine components and systems for testing. The work presented in this paper will be used by the members in the solar group, and will be compared with contractor engine studies. While most of the engine work done to date has been on the blackbody absorber type of engine, the equations presented in this paper can also be applied to other engine types (Reticulated Vitreous Carbon Thruster (RVCT), Beam-Fractionating, et al.).

Tests conducted in the near future will validate AFRL's ability to improve current engine configurations. These tests will demonstrate the STP's ability to operate for extended periods of time under high temperatures and to continually meet/exceed IHPRT goals. IHPRT, Integrated High-Payoff Rocket Propulsion Technology, is the means by which in-house efforts receive funding. Performance goals must be met to continue IHPRT funding. By continually improving the design, engines are continuously and consistently out performing their predecessors.

### Curriculum Vitae

Stephanie Renee Chenault is the test engineer for the Solar Thermal Rocket Propulsion Group located at the Air Force Research Laboratory, Edwards AFB, CA. She received a BS in Aerospace Engineering from Texas A&M University in 1997 and plans on attending the Naval Postgraduate School. Stephanie tests and evaluates all flight-qualified hardware and is involved in engine/thruster research and development for advanced propulsion concepts, specifically those benefiting the warfighter. Other interests include breast cancer awareness and aerospace/astronautics education for high school level young women.